Bioresource Technology 310 (2020) 123454

Contents lists available at ScienceDirect

Bioresource Technology

journal homepage: www.elsevier.com/locate/biortech

Roles of Co-solvents in hydrothermal liquefaction of low-lipid, high-protein algae

Zheng Cui[a], Feng Cheng[b], Jacqueline M. Jarvis[c], Catherine E. Brewer[a], Umakanta Jena[a,*]

[a] Department of Chemical and Materials Engineering, New Mexico State University, Las Cruces, NM 88003, USA
[b] Department of Chemical Engineering, Worcester Polytechnic Institute, MA 01609, USA
[c] Department of Plant and Environmental Sciences, New Mexico State University, Las Cruces, NM 88003 USA

ARTICLE INFO

Keywords:
Crude glycerol
Wastewater treatment algae
Hydrothermal liquefaction
Nitrogen balance

ABSTRACT

Valorization of algal biomass is often limited by its low lipid content. Here, different alcohols: ethanol, isopropanol, and glycerol, were studied as co-solvents to improve the conversion efficiency of a lipid-poor microalgae, *Galdieria sulphuraria,* by hydrothermal liquefaction. Bio-crude oil yield increases, from 13 to 73 wt% (on dry algae basis), were attributed to the alcohols facilitating the transfer of algal protein-derived fragments from the aqueous phase into the oil phase. A series of characterization results showed that bio-crude oil formation was mainly the result of alcohols reacting with algal fragments via Maillard reactions, alkylation, and esterification, respectively. Insights into the synergistic effect of low-lipid feed and alcohol provide mechanistic support for choosing an alcohol-rich waste, crude glycerol, to improve bio-crude oil production from HTL of wastewater-grown *G. sulphuraria*. Promising improvements in yield and energy recovery indicates competitive economics for a low-lipid biomass waste-to-biofuel conversion technique.

1. Introduction

Inedible biomass, such as agricultural, forestry and municipal wastes, have been frequently studied as desirable energy resources to produce environment-friendly biofuels through different routes involving a range of thermal, chemical, and biological processes. Hydrothermal liquefaction (HTL) is one of the promising thermochemical conversion methods for wet biomass since HTL avoids the costs for dewatering and drying (Peterson et al., 2008). As an environmentally-friendly and inexpensive solvent, water has been a common reaction medium under subcritical conditions (180–370 °C, 5–21 MPa). HTL involves acid and based-catalyzed reactions of H^+ and OH^- ions from water (Isa et al., 2018), which lead to degradation and hydrolysis, decarboxylation, repolymerization, deamination, and Maillard reactions to convert the macromolecules in biomass into oil molecules, water-soluble molecules, gas, and char (Peterson et al., 2008).

Microalgae can grow with simple requirements (light, CO_2, water, N, P and K) and provide large capacity for converting CO_2 into biomass and liberating O_2 via photosynthesis (Demirbas, 2011). *Galdieria sulphuraria* is an acidophilic and moderately thermophilic red algae that is regarded as a potential species for wastewater treatment and biofuel energy recovery due to its high nutrient removal efficiencies from urban wastewater (Selvaratnam et al., 2015). To enhance energy recovery, an algae-to-biofuel conversion platform through HTL has been studied. Previous research on HTL of media-grown *G. sulphuraria* showed that more severe conditions (350 °C, 60 min) are required to obtain the highest yield of bio-crude oil (~31 wt%), while the yields of bio-crude oil derived from wastewater-treatment *G. sulphuraria* (WWGS) were lower (~18 wt%) at the optimized condition (Cheng et al., 2019). The quality of bio-crude oils from *G. sulphuraria* is not favorable due to the high protein contents in the algal biomass. Improvements in bio-crude oil yield and quality are needed for WWGS HTL to be feasible.

Many studies have reported that alcohols (e.g. methanol, ethanol, isopropanol, butanol and glycerol) improve the yield and quality of bio-crude oil (Biswas et al., 2017; Yuan et al., 2007). Alcohols have several advantages over water in the HTL process: they (1) provide milder reaction conditions because of their lower critical points (the critical conditions of methanol and ethanol are 239 °C and 8 MPa, and 241 °C and 6 MPa, respectively, compared to water at 374 °C and 22 MPa), (2) have better hydrogen donation ability to stabilize free radicals, (3) can dissolve more molecules into the bio-crude oil phase, and (4) have high reactivity with acidic components to form esters (Zhang and Zhang, 2014). Yuan et al. reported that the oil yield peaked (from 28 wt% to 40 wt%) at a ratio of 50 vol% for ethanol–water/isopropanol-water HTL of rice straw (Yuan et al., 2007). Yu et al. observed the highest oil yield at 40 vol% of ethanol–water for HTL of microalgae *Dunaliella tertiolecta*

* Corresponding author.
E-mail address: ujena@nmsu.edu (U. Jena).

https://doi.org/10.1016/j.biortech.2020.123454
Received 29 January 2020; Received in revised form 24 April 2020; Accepted 25 April 2020
Available online 27 April 2020
0960-8524/

(Chen et al., 2012). Caporgno et al. reported that the highest oil yield was obtained at 50 wt% ethanol-water for HTL of microalgae *Nannochloropsis oceanica* (Caporgno et al., 2016). Feng et al. reported that the oil yield increased significantly for HTL of microalgae when the ethanol-water ratio reached 50 vol% and changed slightly between 50 vol% and 100%, whereas the conversion rate of algae was highest at 50 vol% (Feng et al., 2018). Although Cao et al. indicated the highest oil yield of rice straw occurred at 100% glycerol, the product separation was increasingly difficult, therefore, they concluded 50 vol% was a more appropriate glycerol-water ratio (Cao et al., 2016). These studies emphasized that there were synergistic effects between alcohols and water, especially around a co-solvent/water around 40–50% regardless other conditions for various feedstocks. From an economic perspective, a much high co-solvent ratio is not favorable for the conversion of wet algal feedstock. Hot-compressed water has stronger acidity than ethanol at 200–350 °C, so the addition of water into ethanol enhances the promotion of hydrolysis reactions (Cheng et al., 2012). The presence of some ethanol in water provides better solvation of cracked compounds. Glycerol improved the yield and quality of bio-crude oils from HTL of rice straw (Cao et al., 2016), animal wastes (Ye et al., 2012), and algae (Lu et al., 2017). Lu et al. reported that crude glycerol increased the bio-crude oil yield from 13.4% to 38.7%, and reduced the N content from 3.8% to 1.0% for HTL of low-lipid macroalgae, *Enteromorpha prolifera* (Lu et al., 2017). Only a few studies have provided detailed chemical mechanisms for the interactions between alcohols and biomass during HTL to explain the improvements.

Glycerol as a co-solvent may be more promising for biomass liquefaction because of its lower cost and easy accessibility from renewable sources. Crude glycerol is the major byproduct of the biodiesel industry. In 2016, global production of biodiesel was estimated at 37 billion gallons with co-production of 4 billion gallons of crude glycerol—well exceeding the market demand for glycerol (KumarGarlapati et al., 2016). In 2018, crude glycerol sold at $0.40/kg for refining and $0.11/kg for disposal, while the price of refined glycerol was $1.04–1.10/kg ("Glycerine Market Report," 2018). Current value-added applications for crude glycerol are as animal feed, catalytic chemical conversion, and biotransformation (Yang et al., 2012). Combined, the surplus supply of crude glycerol and the positive outcomes of early work on co-solvent HTL suggest that there is substantial potential of crude glycerol for HTL conversion of wet biomass to liquid fuels.

In this study, we evaluated the effects of alcohol co-solvents (ethanol, isopropanol and glycerol) on bio-crude oil production from HTL of low-lipid wastewater-treatment microalgae, *G. sulphuraria*, in terms of bio-crude oil chemistry. According to the critical temperature and pressure properties of the co-solvent/water mixture, a co-solvent/water ratio of 40 wt% at 310 °C was selected as the initial condition for three co-solvents to keep the mixed solvent sub-critical. Higher temperatures (330 °C and 350 °C) were tested for optimized co-solvent mixtures. This study is providing a comprehensive oil chemistry for clarifying the roles of different alcohol co-solvents on HTL performance of this lipid-poor, protein-rich algae using multiple characterization methods, in particular using a more sensitive, high-resolution analytic instrument Fourier transform mass spectroscopy (FT-MS). To the authors' knowledge, detailed study of co-solvents with this wastewater-grown lipid-poor algae species has not been reported earlier. A feasible low-cost and energy-efficient pathway for low-lipid biomass and industrial wastes to energy-rich biofuel is presented here. The specific objectives of this study were to: (1) evaluate the influence of different alcohols on yield and chemistry of bio-crude oil from *G. sulphuraria*; (2) elucidate possible mechanisms of alcohols for promoting bio-crude oil formation; and (3) investigate the feasibility of an industrial real case: HTL of wastewater algae with crude glycerol, in terms of bio-crude oil yield and energy recovery, according to the synergistic mechanisms between low-lipid algae and alcohols.

2. Materials and methods

2.1. Algae feedstock and co-solvents

Both media-grown and wastewater-grown *G. sulphuraria* algae species were used for HTL. The growth and harvest conditions of media-grown algae *G. sulphuraria* are described in (Cheng et al., 2017). WWGS was cultivated using a 700 L photobioreactor (PBR) fed with primary-settled wastewater at the Jacob A. Hands Wastewater Treatment Plant (Las Cruces, NM). A single PBR was initiated with 400 L of primary wastewater and 300 L pre-adapted algal cultures, where the headspace was filled with 2% CO_2-enriched air (Henkanatte-gedera et al., 2016). Ethanol (5% hydrous), isopropanol, and glycerol (ReagentPlus®, ≥99.0%) were purchased from Sigma-Aldrich. Crude glycerol was provided by Rio Valley Biofuels (El Paso, TX) and used as received. Hexane and acetone were analytical grade (Pharmco-Aaper, Shelbyville, KY).

2.2. Co-hydrothermal liquefaction of microalgae with alcohols

HTL experiments were performed in a 1.8 L Model 4572 stainless steel batch reactor with a Model 4848B controller unit (Parr Instrument Co., Moline, IL). Algae slurries (500 g) with 5 wt% solids concentration were converted at three temperatures (310, 330 and 350 °C) for 30 min with an initial pressure of 1.38 MPa of nitrogen. The alcohols used here included ethanol (EtOH), isopropanol (IPA), glycerol (GLY), and crude glycerol (CGLY). For HTL incorporating ethanol, isopropanol, and glycerol, the mass ratios of alcohol to water were 0 and 40 wt%. For HTL with crude glycerol, the mass ratios were 0 and 100 wt%. Runs at each condition were duplicated. After reaction, the headspace gas was vented. HTL products: bio-crude oil, aqueous phase, and char, were recovered using a hexane extraction procedure, followed by vacuum filtration, Soxhlet extraction with acetone, and then solvent evaporation at 50 °C using a rotary evaporator. The detailed product recovery procedure is described in (Cheng et al., 2018). The hexane-soluble product was designated as light bio-crude oil (LBO); the hexane-insoluble, acetone-soluble fraction was designated as heavy bio-crude oil (HBO).

2.3. Calculation of product and elemental yields, and energy recovery

For HTL in water, ethanol, and isopropanol, product yield was calculated by:

$$Y_i = \frac{W_i}{\text{Dry algae weight}} \times 100\% \quad (1)$$

HTL with glycerol and crude glycerol achieved apparent yields > 100% by Eq. (1), indicating participation of the co-solvent in the reaction. Considering the substantial amount of mass and energy contributed by the co-solvent into the HTL products, an alternative yield calculation was used:

$$Y_i = \frac{W_i}{\text{Dry algal weight} + W_g} \times 100\% \quad (2)$$

where Y_i = yield of product fraction, W_i = weight of product fraction, W_g = weight of organic compounds in glycerol/crude glycerol, and i represents LBO, HBO, char, or non-volatile residue in the aqueous phase.

Energy recovery (ER) of LBO for co-HTL of algae and crude glycerol was calculated by:

$$ER = \frac{Mass\ of\ LBO \times HHV\ of\ LBO}{M_{algae} \times HHV_{algae} + M_{CGLY} \times HHV_{CGLY}} \quad (3)$$

where, M_{algae} and M_{CGLY} were mass of dry algae and dry crude glycerol, respectively, and HHV_{algae} and HHV_{CGLY} were the higher heating values obtained by bomb calorimetry.

The yield of carbon and nitrogen in the products (LBO, HBO and non-volatiles in the aqueous phase) were calculated by:

$$Carbon/nitrogen\ \ yield = \frac{Carbon/nitrogen\ weight\ in\ product}{Carbon/nitrogen\ weight\ in\ algae\ and\ co-solvent} \quad (4)$$

Yield increment ratios for LBO, carbon, and nitrogen, were calculated by:

$$Yield\ increment\ ratio = \frac{Yield\ from\ co-solvent\ HTL}{Yield\ from\ water-HTL} \quad (5)$$

The predicted yield of WW *G. sulphuraria* and crude glycerol was calculated by:

$$Y_{cal} = \frac{Y_W \times C_W + Y_{CG} \times C_{CG}}{C_W + C_{CG}} \times 100\% \quad (6)$$

where Y_W and Y_{CG} are LBO yields when WWGS and crude glycerol were processed by HTL independently, and C_W and C_{CG} is the solids concentration in WWGS and crude glycerol. The predicted energy recovery (ER) of co-HTL of WWGS with crude glycerol were also calculated by Eq. (6), where Y_W and Y_{CG} are replaced by ER_W and ER_{CG}, which are energy recoveries from HTL of WWGS and HTL of crude glycerol, respectively.

2.4. Characterization of feedstocks and HTL products

The methods to measure lipid and carbohydrate contents were mentioned in (Cheng et al., 2018). Methods of feedstock and HTL product characterization were same as previous studies (Cheng et al., 2018, 2017), including moisture content of feedstock and aqueous phase, elemental CHNS content, total organic carbon (TOC) and total nitrogen (TN) of the aqueous phase, higher heating values (HHV) and thermogravimetric analysis (TGA) and chemical functional groups by Fourier transfer infrared spectroscopy (FT-IR). Each sample was analyzed in duplicate or triplicate. Additional characterization method details can be found in (Cheng et al., 2018, 2017).

Heteroatom compound distributions in the bio-crude oils were analyzed by two different Fourier transform mass spectroscopy (FT-MS) instruments as instrument availability allowed. Samples derived from HTL at 310 °C were analyzed with an Orbitrap Fusion mass spectrometer (Thermo Scientific, San Jose, CA) equipped with an Advion TriVersa NanoMate system (Advion, Ithaca, NY). The remaining samples were analyzed using a custom-built 9.4 T FT-ICR mass spectrometer (National High Magnetic Field Laboratory, Tallahassee, FL) (Kaiser et al., 2011). These two instruments are both classified as FT-MS because they use Fourier transform for converting the frequency of ion motion into *m/z*. Sample preparation for positive ion electrospray ionization (ESI), data analysis, and visualization are described in (Cheng et al., 2019; Jarvis et al., 2017).

Bio-crude oils were also characterized using gas chromatography-mass spectrometry (GC–MS, Varian CP-3800, CA, USA) equipped with a ZB-624 column (30 m × 0.25 mm I.D. × 1.4 μm FT). Helium (100 kPa, 1 mL/min) was used as the carrier gas. The injection temperature and interface temperature were 250 °C and 320 °C, respectively. The ion source was adjusted to 230 °C. All chromatogram peaks were compared with electron impact mass spectra from a NIST database. Samples were directly diluted with dichloromethane. The column temperature was set at 40 °C for 0 min, ramped at 5 °C/min to 150 °C for 1 min, then ramped to 200 °C for 1 min, and to 260 °C for 10 min.

3. Results and discussion

3.1. Algae biomass and crude glycerol composition

Algal biomass and crude glycerol characteristics are shown in Table 1. Media-grown *G. sulphuraria* and WWGS had similar elemental and biochemical compositions, except that WWGS contained more ash (14.0 wt% vs. 10.3 wt%) and less lipid (0.3 wt% vs. 6.3 wt%) on a dry basis. The protein and carbohydrate contents were similar: 55.6–57.5 wt% and 27.5–28.7 wt%, respectively. The crude glycerol was a thick, brown slurry containing 14.1 wt% moisture and methanol, 29.1 wt% lipids, and 6.2 wt% ash.

Table 1
Composition of algal feedstocks and crude glycerol.

Algae species	*G. sulphuraria*	WW *G. sulphuraria*	Crude glycerol
Proximate analysis			
Moisture content, wt% [b]	69.0 ± 0.3	83.9 ± 0.3	14.1 ± 0.1
Ash content, wt% [a]	10.3 ± 0.4	14.0 ± 0.4	6.2 ± 0.3
HHV, MJ/kg [a]	27.7 ± 0.3	27.6 ± 0.1	28.9 ± 0.5
Elemental analysis, wt% [a]			
Carbon	44.4 ± 0.2	44.1 ± 0.2	60.4 ± 1.8
Hydrogen	6.1 ± 0.1	5.9 ± 0.1	9.6 ± 0.3
Nitrogen	9.2 ± 0.0	8.9 ± 0.0	0.2 ± 0.0
Sulfur	3.4 ± 0.0	4.0 ± 0.2	2.7 ± 0.3
Oxygen [c]	26.5 ± 0.5	23.2 ± 0.5	20.9 ± 1.9
Biochemical analysis, wt%			
Lipid	6.3 ± 0.1 [a]	0.3 ± 0.0 [a]	29.5 ± 0.1 [b]
Protein [d]	57.5	55.6	–
Carbohydrate [a]	27.5 ± 0.7	28.7 ± 0.2	–

[a] Dry basis.
[b] Wet basis.
[c] By difference.
[d] Calculated by multiplying N content by 6.25 (Mariotti et al., 2008). WW: wastewater-grown.

The differential thermogravimetry (DTG) curves for the feedstocks showed few differences between media-grown *G. sulphuraria* and WWGS, which is consistent with (Cheng et al., 2018). Both had a weight loss maximum between 220 and 320 °C due to the decomposition of protein content. Crude glycerol showed three main stages of weight loss. The first stage at 120–220 °C had a weight loss of approximately 40 wt%, attributed to the decomposition of pure glycerol (Delgado et al., 2013). The second stage (approximately 20 wt% loss) happened at 300–380 °C, which corresponded to the degradation of impurities such as fatty acids methyl esters (Dou et al., 2009). The third stage at 420–460 °C (approximately 10 wt%) was attributed to the continuous degradation of residual impurities, coke, and ash (Dou et al., 2009).

3.2. Effects of alcohols on HTL of media-grown algae

3.2.1. Product yield

The product yields from HTL using the different alcohol co-solvents are shown in Table 2 calculated by Eq. (1). LBO yields were significantly higher (23.7–24.9 wt%) for co-solvent HTL than for water alone (12.9 wt%). This trend in yield is similar to that observed by Ji et al.: bio-crude oil yield increased from 32 wt% to 62 wt% when 50 vol % ethanol–water solvent was used for HTL of *Spirulina* (Ji et al., 2017). No significant difference among yields for the three different co-solvents was found. For GLY-HTL, sticky, “asphalt-like”, oily compounds mixed with char were observed after hexane filtration and prompted extraction with acetone to yield HBO. This indicates that more large molecules with higher aromaticity were produced in GLY-HTL. HTL char yields decreased from 18.0 wt% without co-solvent to 8.0, 11.2, and 6.2 wt% with ethanol, isopropanol, and glycerol, respectively. This suggests that alcohols act as hydrogen donors to stabilize free radicals from algal biomass to suppress condensation, cyclization, and re-polymerization (Hu et al., 2018). The yields of non-volatiles in the aqueous phase of GLY-HTL exceeded 100% when calculated on a dry algae mass basis, indicating that glycerol derivates are incorporated into the aqueous phase. Yields calculated on a dry algae + glycerol mass basis (Eq. (2)) were 59.4–82.1 wt% (Table 2). This indicates that the weight of added co-solvents should be included when calculating product yields

Table 2
Product yields from HTL of media-grown *G. sulphuraria* with water and 40% EtOH/ IPA/ GLY.

Conditions (Solvent, Temperature ° C)	Product yield (wt%) by Eq. (1)				Product yield (wt%) by Eq. (2)			
	LBO	HBO	AP[a]	Char	LBO	HBO	AP[a]	Char
Water, 310	12.9 ± 1.2	–[b]	27.9 ± 0.9	18.0 ± 0.2				
EtOH, 310	23.7 ± 2.3	–[b]	37.1 ± 0.1	8.0 ± 0.0				
IPA, 310	24.9 ± 0.0	–[b]	34.9 ± 0.1	11.2 ± 0.9				
GLY, 310	24.9 ± 0.6	27.6 ± 1.4	705.8 ± 0.6	6.2 ± 0.0	2.9 ± 0.0	3.2 ± 0.1	82.1 ± 0.1	0.7 ± 0.0
GLY, 330	31.6 ± 4.3	43.0 ± 0.0	643.6 ± 2.8	10.0 ± 0.0	3.7 ± 0.4	5.0 ± 0.0	74.9 ± 0.3	1.2 ± 0.0
GLY, 350	73.2 ± 0.1	23.1 ± 1.8	510.9 ± 0.3	4.0 ± 0.6	8.8 ± 0.2	3.1 ± 0.4	59.4 ± 0.0	0.5 ± 0.1

[a] Non-volatile residue in aqueous phase. EtOH: ethanol. IPA: isopropanol. GLY: glycerol. LBO: light bio-crude oil. HBO: heavy bio-crude oil. AP: aqueous phase.
[b] No HBO produced.

for alcohols in HTL. With increasing temperature, yields of non-volatiles in the aqueous phase decreased from 82.1 to 59.4 wt%, indicating that compounds initially dissolved in the aqueous product were converted into the oil phase with increasing temperature (Gai et al., 2015; Han et al., 2019).

Based on the highest LBO and HBO yields (on a dry algae basis), glycerol was the most effective HTL co-solvent. As the temperature increased to 350 °C, LBO yield from GLY- HTL increased from 24.9 to 73.2 wt% on a dry algae basis (Table 2), and from 2.9 to 8.8 wt% on dry algae + glycerol basis. This is consistent with a previous observation that high temperature favors bio-crude oil formation from pure glycerol (Maglinao and He, 2009).

3.2.2. Carbon and nitrogen recoveries in HTL products

Table 3 shows the carbon and nitrogen yields in the oil, aqueous phase, and char phases calculated by Eq. (4). The higher carbon yield in the aqueous phase from co-solvent HTL (48.5–90.1 wt% vs. 37.9 wt% for water alone) suggests that much of the added co-solvent contributes to the aqueous phase. Carbon yield in the char phase decreased to 0.1–0.2 wt%, supporting the hypothesis that co-solvent inhibits the formation of char. Nitrogen in HTL products was expected to derive exclusively from the algae feedstock, therefore, any N-containing compounds found to increase in the LBO phase were considered evidence of how alcohols improve bio-crude oil yield. Here, the N content in LBO from co-solvent HTL did not change substantially (3.1–5.9 wt%) from the 4.7 wt% N content in the LBO from water HTL. In terms of yield, N was enriched in the LBO with co-solvent (7.1–14.4 wt%) compared to that without co-solvent (6.0 wt%) at 310 °C. Simultaneously, N fractionation into the aqueous and char phases decreased as co-solvent was used compared to water used alone. The increase in N yield for GLY-HTL (from 11.7 wt% to 37.7 wt%) was attributed to the more severe reaction conditions. When Eq. (5) was used, there was a strong polynomial relationship between mass yield of LBO and N yield in LBO, suggesting that the increase in bio-crude oil yield was from the greater participation of protein-derived amino acids participation with co-solvent during HTL rather than co-solvent reacting alone and transferring into the oil phase.

At the lower temperature (310 °C), GLY-LBO C and H contents increased (78.7 vs. 78.5 wt%, 10.4 vs. 9.7 wt%), and N and O contents decreased slightly (4.4 vs. 4.7 wt%, 3.5 vs. 3.6 wt%) compared with water-LBO. With more severe conditions, the C and H content decreased while N and O were enriched in GLY-LBO. GLY-HBO had much lower C and H contents (53.4 vs. 70.7 wt% and 7.0 vs. 7.6 wt%) and higher O content (15.3 vs. 34.0 wt%) compared to GLY-LBO. GLY-HBO had a significantly high viscosity and was hard to collect as a liquid, properties that would make it more difficult to upgrade to high-quality liquid biofuel than LBO.

3.2.3. Bio-crude oil composition by FT-MS and GC–MS

Heteroatom class distribution in LBO (positive-ion ESI mode FT-MS) from HTL with and without co-solvent at 310 °C are shown in Fig. 1(a). Generally, N_1, N_1O_1, N_2, and N_2O_1 were the dominant species for all four bio-crude oils, which total relative abundance (RA) was > 50%. Isoabundance-color contour plots of double bond equivalent (DBE) vs. carbon number for positive-ion ESI are shown in Fig. 2. The distribution of peak areas from different compound classes by GC–MS is shown in Table 4. The combination of GC–MS and FT-MS enable more insight into the mechanisms of co-solvent effects in HTL by allowing comparison of both the low-molecular-weight volatile compounds and the non-volatile compounds in LBO.

3.2.3.1. Effects of ethanol and isopropanol. Water-LBO, EtOH-LBO, and IPA-LBO have similar color-coded abundance–contoured plots (Fig. 2(a)). N_1 species in these three LBO vary widely from $C_{7\text{-}40}$ and DBE of 0–16. The most abundant N_1 species have carbon numbers of 9–11 and a DBE of 1, which most likely correspond to alkyl amines and cyclic secondary amines from the degradation of amino acids (Sudasinghe et al., 2014). The N_1O_1 species, with carbon numbers of 16–22 and DBE of 0–4, are most likely fatty acid amides; the species with high DBE correspond to aromatic amides and heteroaromatic structures such as pyrrole, indole, and carbazole (Sudasinghe et al., 2014). Although the total relative abundance of the N_1O_1 class in EtOH-LBO was less than that of the water-LBO, the relative abundance of N_1O_1 species with carbon numbers of 16–22 and DBE of 0–4 in EtOH-

Table 3
Carbon and nitrogen yields in HTL products.

Condition (Solvent, Temperature °C)	Carbon yield, wt%					Nitrogen yield, wt%				
	LBO	HBO	AP	Char	Gas & Loss [a]	LBO	HBO	AP	Char	Gas & Loss [a]
Water, 310	20.7	-[b]	37.9	4.9	36.6	6.0	-[b]	72.5	4.1	17.4
EtOH, 310	3.1	-[b]	64.7	0.1	32.1	7.1	-[b]	13.3	1.6	78.1
IPA, 310	3.8	-[b]	48.5	0.2	47.8	14.4	-[b]	13.3	2.2	70.0
GLY, 310	5.6	4.1	90.1	0.1	0.1	11.7	8.7	17.2	1.1	61.3
GLY, 330	7.7	8.5	81.1	0.1	2.5	23.0	25.0	31.3	1.6	19.1
GLY, 350	15.5	4.4	72.0	0.1	8.0	37.7	10.4	43.4	2.5	6.0

[a] By difference. LBO: light bio-crude oil. HBO: heavy bio-crude oil. AP: aqueous phase. EtOH: ethanol. IPA: isopropanol. GLY: glycerol. CGLY: crude glycerol.
[b] No HBO produced.

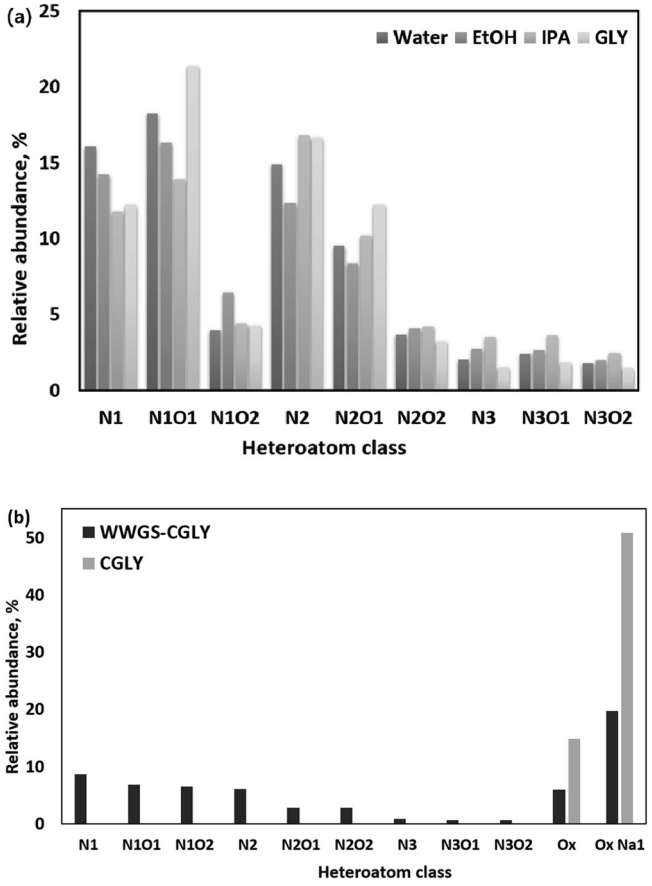

Fig. 1. Heteroatom class distribution of (a) LBOs obtained from HTL with water alone, 40 wt% EtOH, 40 wt% IPA, and 40 wt% GLY at 310 °C; (b) LBOs from CGLY and WWGS-CGLY at 350 °C. All samples were derived from positive-ion ESI FT-MS. EtOH: ethanol, IPA: isopropanol, GLY: glycerol, WWGS: wastewater-treatment *G. sulphuraria*, CGLY: crude glycerol.

LBO (3.6%) was higher than that in water-LBO (2.6%). These compounds are most likely to be fatty acid amides formed by the condensation of fatty acids and ammonia (Sudasinghe et al., 2015). Ammonia is produced from the deamination of amino acids under hydrothermal conditions (Sato et al., 2004). The "hotspot" of N_1O_1 species from EtOH-LBO (Fig. 2(a)) is $C_{18}H_{37}N_1O_1$ with a DBE of 1, which is expected to be octadecanamide from the reaction of octadecanoic acid with ammonia. N_1O_2 species with carbon numbers of 21–24 and DBE of 2 are more concentrated in EtOH-LBO and IPA-LBO than in water-LBO, and likely represent unsaturated alkyl-chain amides. This suggests that the alcohol accelerates the formation of alkylated fatty acid amides. The most abundant formula of the N_1O_2 class in EtOH-LBO was $C_{20}H_{33}N_1O_2$ with a DBE of 5 (0.95% of the total RA). Interestingly, water-LBO had a "hotspot" for the N_1O_2 class at a carbon number of 18 with a DBE of 5 ($C_{18}H_{29}N_1O_2$). This represents compounds with the same DBE but a shift in carbon number by + 2, indicating that $C_{20}H_{33}N_1O_2$ in EtOH-LBO is likely the ethyl-alkylated version of $C_{18}H_{29}N_1O_2$ from water-LBO. At a DBE of 4, the "hotspots" in water-LBO for the N_2 and N_2O_1 classes are $C_8H_{12}N_2$, $C_{10}H_{16}N_2O_1$, and $C_{11}H_{18}N_2O_1$, respectively, while the "hotspots" for EtOH-LBO are again higher in carbon number by 2 ($C_{10}H_{16}N_2$, $C_{12}H_{20}N_2O_1$ and $C_{13}H_{22}N_2O_1$), which are likely alkyl-pyrazines and oxygenated alkyl-pyrazines (Sudasinghe et al., 2014). This may indicate that $C_8H_{12}N_2$, $C_{10}H_{16}N_2O_1$, and $C_{11}H_{18}N_2O_1$ are alkylated by ethanol. Ethanol has been used as a capping agent to stabilize intermediates by alkylating aromatic rings to suppress repolymerization (Huang et al., 2015).

The most abundant compound for the N_1O_2 class in IPA-LBO had a carbon number of 21 and a DBE of 5 ($C_{21}H_{35}N_1O_2$), three carbons more than $C_{18}H_{29}N_1O_2$ from water-LBO. This may indicate a similar mechanism of alkylation of N_1O_2 species by isopropanol. N_2O_1 species with carbon numbers > 40 and DBE of 0–3 were observed in EtOH-LBO and IPA-LBO but not in water-LBO. This suggests that long-chain, non-aromatic compounds accumulate in LBO in the presence of ethanol and isopropanol, which may be the result of intramolecular condensation of amino acids (Chiavari and Galletti, 1992). The RA of N_2O_{0-3} and N_3O_{0-3} classes in IPA-LBO were higher than those in water-LBO. Wu et al. found that the presence of alcohols accelerate Maillard reactions and favor the formation of imidazoquinolines (Wu et al., 2011). Such an acceleration was observed here for the N_3O_{0-3} classes in EtOH-LBO and IPA-LBO. The proposed molecules within the N_3O_x classes are alkylated amino-imidazopyridines and amino-imidazoquinoline (Wu et al., 2011).

Esterification of ethanol and isopropanol with fatty acids was observed in the GC–MS spectra. This has been reported by others (Yuan et al., 2007). The peak area fraction for fatty acid esters in EtOH-LBO and IPA-LBO were 41.8% and 16.1%, respectively, higher than the 5.1% for water-LBO (Table 4). Hexadecanoic acid ethyl ester ($C_{18}H_{36}O_2$, 10.0%) and octadecanoic acid ethyl ester ($C_{20}H_{40}O_2$, 3.5%) were identified in EtOH-LBO. Hexadecenoic acid isopropyl ester ($C_{19}H_{38}O_2$, 3.5%) was identified in IPA-LBO. None of these were observed in water-LBO. This indicates that esterification of alcohols with fatty acids occurred in HTL.

3.2.3.2. Effect of glycerol. The heteroatom distribution in GLY-LBO were quite different from those found in EtOH-LBO or IPA-LBO, suggesting different mechanisms during HTL. The degradation pathways of glycerol in sub/supercritical water follow a series of ionic and free radical reactions, whose main products are methanol, ethanol, acetaldehyde, acrolein, allyl alcohols, formaldehyde, and hydrogen (Bühler et al., 2002). The RA for N_1O_1, N_2, and N_2O_1 classes in GLY-LBO were much higher than those in water-LBO (Fig. 1(a)). The four most abundant compounds were $C_8H_{12}N_2$, $C_9H_{14}N_2$, $C_7H_{10}N_2$, and $C_{10}H_{16}N_2$ (1.25%, 0.92%, 0.73% and 0.73 % RA, respectively), which could correspond to alkylated pyrazines. According to GC–MS results reported by Gai et al. and Lojzova et al., $C_8H_{12}N_2$, $C_9H_{14}N_2$, $C_7H_{10}N_2$, and $C_{10}H_{16}N_2$ are diethyl-pyrazine, methyl-isobutyl-pyrazine, ethyl-methyl-pyrazine, and dimethyl-isobutyl-pyrazine from Maillard reactions (Gai et al., 2015). These compounds represent nitrogenous organic compounds in the aqueous phase from HTL of low-lipid algae (Gai et al., 2015). This suggests that co-solvent helps in the transfer of water-soluble compounds into the oil phase. Cerny et al. reported that a proportion of glycerol carbon is in the form of pyrazines (Cerny and Guntz-dubini, 2006). The oxidation products of glycerol, such as 2-oxopropanal and hydroxy-2-propanone, are important precursors that react with amino acids to produce pyridines and pyrrolines through Maillard reactions (Smarrito-menozzi et al., 2013). Such reaction products correspond to the higher abundance of N_1O_1 compounds with carbon numbers of 9–12 and DBE of 2–3 in GLY-LBO. The abundance of N_1O_2 species with DBE of < 4 was higher in GLY-LBO than in water-LBO, indicating that formation of unsaturated fatty acid amides was favored in the presence of glycerol. The N_2O_1 class of GLY-LBO showed a high abundance of species with a DBE of 4–7, whereas species with DBE of 7 were not as prominent in the water-LBO. The N_2O_1 species with DBE of 7 are most likely quinazolinone derivatives (Jarvis et al., 2017). The presence of glycerol provides an efficient way to form quinazolinone derivatives from aminobenzamides condensed with aldehydes and ketones (Reza et al., 2013). These mechanisms may explain the higher RA of N_1O_1, N_2, and N_2O_1 classes in GLY-LBO compared with those in water-LBO.

By GC–MS, fatty acid esters were not observed in GLY-LBO. One possibility is that fatty-acid-glycerol esters could not be detected due to the limitations of GC–MS based on compound volatility/stability at analysis temperatures. The N yield (Table 3) showed that many algae-derived fragments were transferred into the oil phase during co-solvent

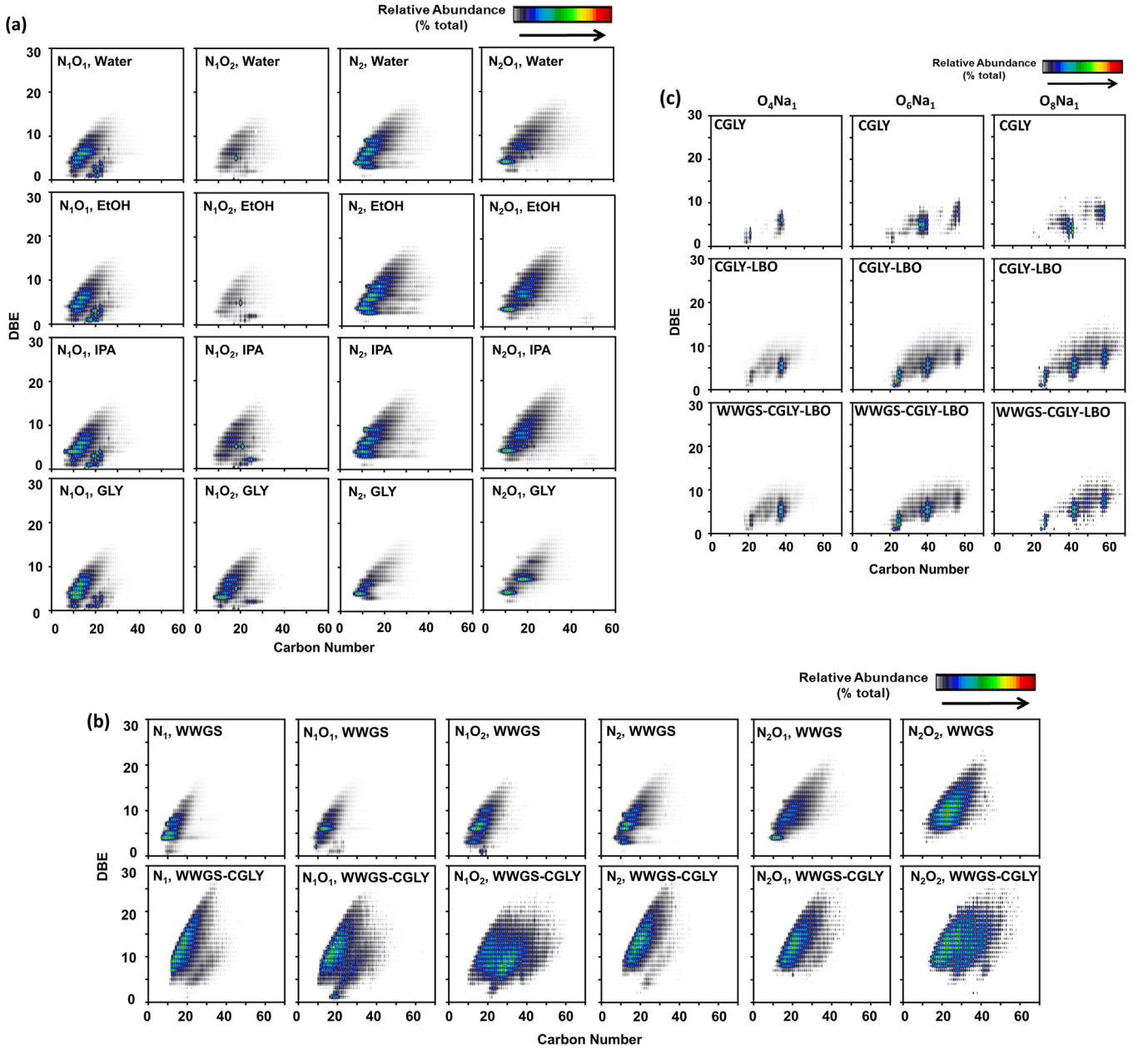

Fig. 2. (a) Color-coded abundance–contoured plots showing double bond equivalent (DBE) vs. carbon number for heteroatom classes (a) in LBOs from water alone and from 40% co-solvents under 310 °C; (b) in LBO of WWGS (Cheng et al., 2019) and WWGS-CGLY under 350 °C; (c) in crude glycerol (no HTL) and LBOs of CGLY and WWGS-CGLY under 350 °C. All samples were derived from positive-ion ESI FT-MS. EtOH: ethanol, IPA: isopropanol, GLY: glycerol, WWGS: wastewater-treatment G. sulphuraria, CGLY: crude glycerol.

Table 4
GC–MS peak area distribution in light bio-crude oils from water alone and 40 wt% co-solvent HTL of *G. sulphuraria* at 310 °C.

Conditions (Solvent type)	Peak area, %						
	Fatty acid esters	Hydro-carbons	N-containing	N&O-containing	Alcohols & phenols	Ketones & aldehydes	Acids & acetates
Water	5.1	30.4	16.4	2.5	18.4	17.8	5.0
EtOH	41.8	18.3	12.1	4.5	12.6	9.0	2.0
IPA	16.1	28.8	16.9	6.0	19.5	10.9	2.2
GLY	0.0	19.4	15.7	7.6	36.4	14.7	3.2

EtOH: ethanol, IPA: isopropanol, GLY: glycerol.

HTL, which would decrease the concentration of such esters. Also, esterification of glycerol may not possibly occur due to the competition between fatty acids and protein-derived compounds for reaction with glycerol. The peak area fraction for other O-containing compounds in GLY-LBO, such as derivatives of alcohol, phenol, ketone, aldehyde, acid, and acetate, was 54.3%, much higher than for the other three LBO samples. This may be the result of degradation of glycerol, followed by dehydration and condensation with small fragments from algae (Tendam and Hanefeld, 2011).

3.2.4. Bio-crude oil characterization by FT-IR

Peaks for N—H stretching (3400–3200 cm^{-1}), C—H stretching (2957, 2924 and 2854 cm^{-1}), C═O (1710–1671 cm^{-1}), C—H bending (1456 and 1379 cm^{-1}), and C(aromatic)-H out-of-plane bending (803–700 cm^{-1}) were found in all spectra for LBO and indicate the presence of hydrocarbons, fatty acids, amides, and N&O-heteroatom aromatic compounds. The typical carbonyl group (C═O) stretching vibration between 1739 and 1665 cm^{-1} indicates the presence of esters, ketones, or carboxylic acids (Yang et al., 2016). In the spectrum of LBO obtained from EtOH-HTL, the peak around 1739 cm^{-1} is attributed to fatty acid esters, whereas the peak between 1703 cm^{-1} and 1667 cm^{-1} in all four spectra may be due to ketones or fatty acid amides (Biswas et al., 2017). In the spectra for IPA-LBO, the strong peak at 1667 cm^{-1} most likely indicates cyclic amides and/or carbonyl compounds produced by amination, rearrangement, and Maillard reactions of proteins and carbohydrates in *G. sulphuraria* (Zhang et al., 2016). The bands for C—O stretching (between 1300 cm^{-1} and 1000 cm^{-1}) were much stronger in EtOH-HTL than for the other three, implying the formation of ether groups in EtOH-LBO by dehydration and condensation between ethanol and biomass fragments (Chen et al., 2012). Water-LBO, IPA-LBO, and EtOH-LBO have stronger intensities at the peaks between 800 cm^{-1} and 700 cm^{-1}, indicating the presence of more aromatic rings (Chen et al., 2012). The strong peak for trans═C—H out-of-plane bending (955 cm^{-1}) appears in the spectra for IPA-LBO and GLY-LBO, but it is barely detectable in water-LBO and EtOH-LBO. This may indicate that the addition of glycerol or isopropanol favors the production of unsaturated aliphatic compounds over aromatic compounds. The peak at 1510 cm^{-1} disappears in the GLY-LBO spectrum, which suggests a decrease in C═N from imines and/or C═C from aromatic structures (Cao et al., 2016). Overall, LBO composition by FT-IR varies only slightly with and without co-solvents. Ethanol promotes formation of more ethers, esters, and para-aromatic structures (Biswas et al., 2017), while glycerol and isopropanol produce more ketones and trans-alkene structures.

Compared with GLY-LBO made under the same conditions, the spectrum for GLY-HBO showed a boarder peak for O—H/N—H stretching (3400–3200 cm^{-1}) and stronger peaks for C═O stretching (1709 cm-1), C—C stretching (1605–1551 cm^{-1}), and C—O stretching (between 1300 cm^{-1} and 1000 cm^{-1}). This indicates that HBO had a greater abundance of heteroatom-containing compounds.

3.2.5. Discussion of reaction mechanisms

A possible mechanism for the increased yield of bio-crude oil from HTL of low-lipid algae with alcohol co-solvents is described in Fig. 3 based on (Gai et al., 2015). Compounds highlighted by gray-dashed lines indicate organic compounds that accumulated in the bio-crude oil in the presence of alcohols in HTL. Esterification of fatty acids is the primary reaction for ethanol and isopropanol co-solvent (from GC–MS results). Ethanol, isopropanol, and glycerol show similar mechanisms for accelerating Maillard reactions to form more hydrophobic compounds that enter the oil phase. Ethanol can act as a capping agent to stabilize aromatic rings and suppress repolymerization. Glycerol has a more complex mechanism because its degradation products can participate in Maillard and condensation reactions with algae fragments, such as pyrazines and oxygenated-pyridines. Dehydration and condensation of glycerol with protein fragments introduce more O-containing and oxygenated N-containing compounds into LBO.

3.3. Hydrothermal liquefaction of wastewater-grown G. Sulphuraria with crude glycerol

The predicted and experimental LBO yield and energy recovery for HTL of WWGS and crude glycerol are compared. LBO yields for HTL at 350 °C for 30 min of 5 wt% WWGS in water and of crude glycerol (CGLY) alone were 10.8 wt% (Cheng et al., 2019) and 58.1 wt%, respectively. HTL of a 5 wt% algae and crude glycerol mixed slurry produced 66.2 wt% LBO—higher than the predicted value if algae or crude glycerol were processed independently (Eq. (6)). Energy recovery (calculated by Eq. (3)) for HTL of WWGS with crude glycerol was also higher than predicted (84.5% vs. 69.3%). This indicates a synergetic effect as more organics from algae and crude glycerol are converted into the oil phase. The synergistic yield and energy recovery effects observed for HTL of WWGS with crude glycerol are important to the feasibility of implementation. The high bio-crude oil yields from WWGS and CGLY suggest a promising outlook for these two abundant and low-cost raw materials for more economic biofuels.

N content in the LBO was as low as 0.9 wt%, while the N yield was as high as 71.3 wt% (Eq. (4)). The lower N content in the bio-crude oil may have been caused by dilution with abundant organic compounds derived from the crude glycerol. Oxygen content for LBO from CGLY alone or from WWGS-CGLY were much higher (13.2–14.6 wt%) than for LBO from HTL with purified glycerol, resulting in a HHV as low as 36.8 MJ/kg. The high O content was attributed to the fatty acids in the crude glycerol.

From GC–MS, crude glycerol contains abundant fatty acid methyl esters: 88.1% of the total peak area was from hexadecanoic acid methyl ester ($C_{17}H_{34}O_2$), 9-octadecenoic acid (Z) methyl ester ($C_{19}H_{36}O_2$), and octadecanoic acid methyl ester ($C_{19}H_{38}O_2$), besides methanol and glycerol. The distribution of heteroatom classes also showed that the relative abundance of O-containing species (O_x and O_xNa_1 species, where × ranged from 1 to 15) occupied 64.0% in crude glycerol. The high number of O atoms in these species indicates that crude glycerol contained abundant polymerized O-containing compounds. Fig. 1(b) shows the high relative abundance distribution of O-containing classes (O_x species 14.8% and O_xNa_1 species 50.8%) in LBO from HTL of CGLY alone at 350 °C for 30 min for positive-ion ESI. LBO from co-HTL of WWGS and CGLY showed several N-containing species which were common in algae-derived bio-crude oil, as well as abundant O-substituted compounds (O_x species 5.9% and O_xNa_1 species 19.6%, where × ranged from 1 to 10) derived from crude glycerol, which were hardly observed in LBO from HTL of wastewater algae alone (Cheng et al., 2019, 2017). The color-coded abundance–contoured plots of DBE vs. carbon number for several heteroatom classes in LBO from WWGS alone and WWGS-CGLY, generated under the same reaction conditions, are shown in Fig. 2(b). The data of LBO from WWGS were collected on an Orbitrap Fusion mass spectrometer (Cheng et al., 2019), whereas the WWGS-CGLY were collected on a FT-ICR mass spectrometer. The $N_{1\text{-}2}O_{0\text{-}2}$ classes in LBO from co-HTL of WWGS and CGLY had larger compositional spaces than those from HTL of WWGS alone. The greater diversity of O-substituted, N-containing compounds (carbon number 10–70 and DBE of 0–27) observed in LBO of co-HTL of WWGS and CGLY indicates an alkylation reaction occurred between long-chain compounds from crude glycerol and N-containing compounds from algae.

Fig. 2(c) provides the color-coded abundance–contoured plots of DBE vs. carbon number for several O_xNa_1 (x = 4, 6 and 8) compound classes in crude glycerol before HTL, LBO from HTL of CGLY alone, and LBO from co-HTL of WWGS and CGLY. In each class, the compositional spaces and “hotspot” areas look similar between two the LBO, which suggests that these species did not change during HTL with algae. Comparing the “hotspot” of $C_{37}H_{64}O_4Na_1$ in crude glycerol before HTL with $C_{40}H_{70}O_6Na_1$ in LBO from HTL of CGLY alone and co-HTL of

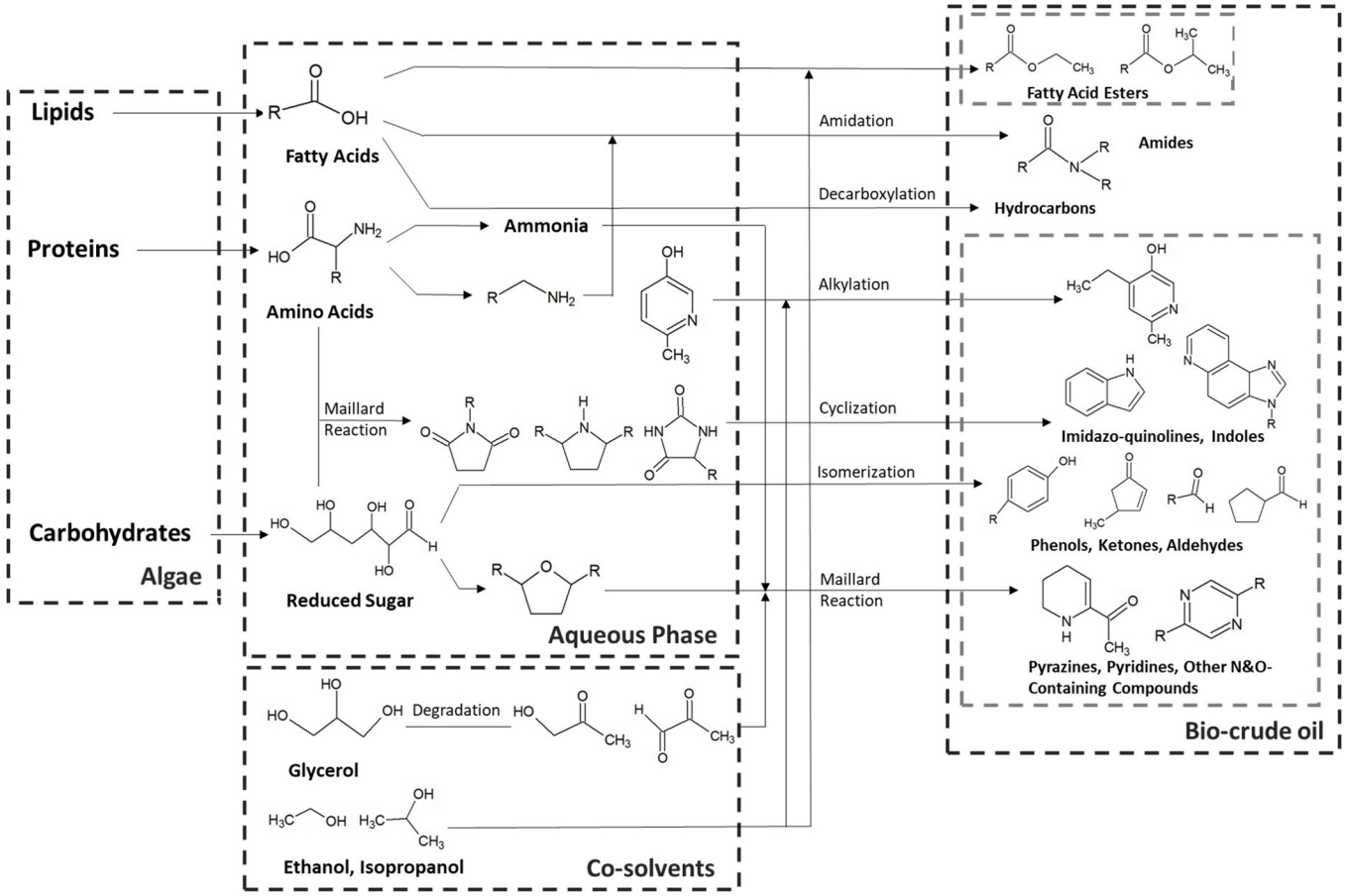

Fig. 3. Possible reaction pathways of algae and alcohols in HTL.

WWGS and CGLY, the first formula has the same DBE (6) of the second formula with differences of 3 C and 2 O atoms. Similar shifts were also observed for $C_{21}H_{40}O_6Na_1$, $C_{37}H_{66}O_6Na_1$, $C_{57}H_{100}O_6Na_1$ in crude glycerol and $C_{24}H_{46}O_8Na_1$, $C_{40}H_{72}O_8Na_1$, and $C_{60}H_{106}O_8Na_1$ in the two LBO. This shift may predict that the condensation or esterification of glycerol occurs during HTL (Lu et al., 2017) to generate the compounds in the O_6Na_1 class, simultaneously removing H_2O to form compounds in the O_8Na_1 class during HTL.

4. Conclusion

Alcohol co-solvents improve bio-crude oil production from algae through promotion of the transfer of N-containing organic compounds into the oil phase. Ethanol and isopropanol promote esterification and Maillard reactions. Glycerol plays an important role as both a co-solvent and as a reactant with algal fragments in Maillard reactions. Crude glycerol acts as a high-lipid additive and an extractant to improve conversion of low-lipid algae feedstock into liquid fuels. Further understanding of the synergistic effects between low-lipid algae and alcohols, and results from co-HTL of two waste streams, crude glycerol and wastewater-grown algae, provide evidence for the technical feasibility of a comprehensive low-cost and high-energy recovery system for low-lipid biomass to biofuels.

CRediT authorship contribution statement

Zheng Cui: Methodology, Data curation, Writing - original draft. **Feng Cheng:** Writing - review & editing. **Jacqueline M. Jarvis:** Data curation, Writing - review & editing. **Catherine E. Brewer:** Supervision, Writing - review & editing. **Umakanta Jena:** Supervision, Conceptualization, Writing - review & editing.

Declaration of Competing Interest

The authors declare that they have no known competing financial interests or personal relationships that could have appeared to influence the work reported in this paper.

Acknowledgements

The authors acknowledge funding from the U.S. National Science Foundation (NSF) “ReNUWIT” Energy Research Center [#1028968], the NSF New Mexico EPSCOR “Energy New Mexico” grant [#1301346], an NSF Major Research Instrumentation grant [#1626468], and a grant from the New Mexico Water Resource Research Institute. A portion of this work was performed at the National High Magnetic Field Laboratory, which is supported by NSF Cooperative Agreement #DMR-1644779, the State of Florida, and the U.S. Department of Energy. The authors acknowledge FT-MS data assistance from the Center for Animal Health and Food Safety at NMSU and the National High Magnetic Field Laboratory. The authors also acknowledge assistance from members of the Holguin, Van Voohries, Khandan, Schaub, and Brewer research groups for algae production, harvesting, conversion, and characterization.

Appendix A. Supplementary data

Supplementary data to this article can be found online at https://doi.org/10.1016/j.biortech.2020.123454.

References

Biswas, B., Arun Kumar, A., Bisht, Y., Singh, R., Kumar, J., Bhaskar, T., 2017. Effects of temperature and solvent on hydrothermal liquefaction of Sargassum tenerrimum algae. Bioresour. Technol. 242, 344–350. https://doi.org/10.1016/j.biortech.2017.03.045.

Bühler, W., Dinjus, E., Ederer, H.J., Kruse, A., Mas, C., 2002. Ionic reactions and pyrolysis of glycerol as competing reaction pathways in near- and supercritical water. J. Supercrit. Fluids 22, 37–53. https://doi.org/10.1016/S0896-8446(01)00105-X.

Cao, L., Zhang, C., Hao, S., Luo, G., Zhang, S., Chen, J., 2016. Effect of glycerol as co-solvent on yields of bio-oil from rice straw through hydrothermal liquefaction. Bioresour. Technol. 220, 471–478. https://doi.org/10.1016/j.biortech.2016.08.110.

Caporgno, M.P., Pruvost, J., Legrand, J., Lepine, O., Tazerout, M., Bengoa, C., 2016. Hydrothermal liquefaction of Nannochloropsis oceanica in different solvents. Bioresour. Technol. 214, 404–410. https://doi.org/10.1016/j.biortech.2016.04.123.

Cerny, C., Guntz-dubini, R., 2006. Role of the solvent glycerol in the maillard reaction of D-fructose and L-alanine. J. Agric. Food Chem. 54, 574–577.

Chen, Y., Wu, Y., Zhang, P., Hua, D., Yang, M., Li, C., Chen, Z., Liu, J., 2012. Direct liquefaction of Dunaliella tertiolecta for bio-oil in sub/supercritical ethanol-water. Bioresour. Technol. 124, 190–198. https://doi.org/10.1016/j.biortech.2012.08.013.

Cheng, F., Cui, Z., Chen, L., Jarvis, J., Paz, N., Schaub, T., Nirmalakhandan, N., Brewer, C.E., 2017. Hydrothermal liquefaction of high- and low-lipid algae: bio-crude oil chemistry. Appl. Energy 206, 278–292. https://doi.org/10.1016/j.apenergy.2017.08.105.

Cheng, F., Cui, Z., Mallick, K., Nirmalakhandan, N., Brewer, C.E., 2018. Hydrothermal liquefaction of high- and low-lipid algae: Mass and energy balances. Bioresour. Technol. 258, 158–167. https://doi.org/10.1016/j.biortech.2018.02.100.

Cheng, F., Mallick, K., Gedara, S.M.H., Jarvis, J.M., Schaub, T., Jena, U., Nirmalakhandan, N., Brewer, C.E., 2019. Hydrothermal liquefaction of galdieria sulphuraria grown on municipal wastewater. Bioresour. Technol. 121884. https://doi.org/10.1016/j.biortech.2019.121884.

Cheng, S., Wilks, C., Yuan, Z., Leitch, M., Xu, C., 2012. Hydrothermal degradation of alkali lignin to bio-phenolic compounds in sub/supercritical ethanol and water-ethanol co-solvent. Polym. Degrad. Stab. 97, 839–848. https://doi.org/10.1016/j.polymdegradstab.2012.03.044.

Chiavari, G., Galletti, G.C., 1992. Pyrolysis-gas chromatography/mass spectrometry of amino acids. J. Anal. Appl. Pyrolysis 24, 123–137. https://doi.org/10.1016/0165-2370(92)85024-F.

Delgado, R., Guillermo, J., Gómez, N., Martínez, O., Elena, M., Cara, J., 2013. Energy valorisation of crude glycerol and corn straw by means of slow co-pyrolysis: production and characterisation of gas, char and bio-oil. Fuel 112, 31–37. https://doi.org/10.1016/j.fuel.2013.05.005.

Demirbas, M.F., 2011. Biofuels from algae for sustainable development. Appl. Energy 88, 3473–3480. https://doi.org/10.1016/j.apenergy.2011.01.059.

Dou, B., Dupont, V., Williams, P.T., Chen, H., Ding, Y., 2009. Thermogravimetric kinetics of crude glycerol. Bioresour. Technol. 100, 2613–2620. https://doi.org/10.1016/j.biortech.2008.11.037.

Feng, H., Zhang, B., He, Z., Wang, S., Salih, O., Wang, Q., 2018. Study on Co-liquefaction of spirulina and spartina alterniflora in ethanol-water Co-solvent for bio-oil. Energy. https://doi.org/10.1016/j.energy.2018.02.146.

Gai, C., Zhang, Y., Chen, W.T., Zhang, P., Dong, Y., 2015. An investigation of reaction pathways of hydrothermal liquefaction using Chlorella pyrenoidosa and Spirulina platensis. Energy Convers. Manag. 96, 330–339. https://doi.org/10.1016/j.enconman.2015.02.056.

Glycerine Market Report, 2018. , in: 5th Global Glycerine Conference.

Han, Y., Hoekman, S.K., Cui, Z., Jena, U., Das, P., 2019. Hydrothermal liquefaction of marine microalgae biomass using co-solvents. Algal Res. 38, 101421. https://doi.org/10.1016/j.algal.2019.101421.

Henkanatte-gedera, S.M., Selvaratnam, T., Karbakhshravari, M., Myint, M., Nirmalakhandan, N., Voorhies, W. Van, Lammers, P.J., 2016. Removal of dissolved organic carbon and nutrients from urban wastewaters by Galdieria sulphuraria: Laboratory to field scale demonstration. ALGAL 24, 450–456. https://doi.org/10.1016/j.algal.2016.08.001.

Hu, Y., Feng, S., Bassi, A., Xu, C.C., 2018. Improvement in bio-crude yield and quality through co-liquefaction of algal biomass and sawdust in ethanol-water mixed solvent and recycling of the aqueous by-product as a reaction medium. Energy Convers. Manag. 171, 618–625. https://doi.org/10.1016/j.enconman.2018.06.023.

Huang, X., Korányi, T.I., Boot, M.D., Hensen, E.J.M., 2015. Ethanol as capping agent and formaldehyde scavenger for efficient depolymerization of lignin to aromatics. Green Chem. 17, 4941–4950. https://doi.org/10.1039/c5gc01120e.

Isa, K.M., Abdullah, T.A.T., Ali, U.F.M., 2018. Hydrogen donor solvents in liquefaction of biomass: a review. Renew. Sustain. Energy Rev. 81, 1259–1268. https://doi.org/10.1016/j.rser.2017.04.006.

Jarvis, J.M., Billing, J.M., Hallen, R.T., Schmidt, A.J., Schaub, T.M., 2017. Hydrothermal liquefaction biocrude compositions compared to petroleum crude and shale oil. Energy and Fuels 31, 2896–2906. https://doi.org/10.1021/acs.energyfuels.6b03022.

Ji, C., He, Z., Wang, Q., Xu, G., Wang, S., Xu, Z., Ji, H., 2017. Effect of operating conditions on direct liquefaction of low-lipid microalgae in ethanol-water co-solvent for bio-oil production. Energy Convers. Manag. 141, 155–162. https://doi.org/10.1016/j.enconman.2016.07.024.

Kaiser, N.K., Quinn, J.P., Blakney, G.T., Hendrickson, C.L., Marshall, A.G., 2011. A novel 9.4 tesla FTICR mass spectrometer with improved sensitivity, mass resolution, and mass range. J. Am. Soc. Mass Spectrom. 22, 1343–1351. https://doi.org/10.1007/s13361-011-0141-9.

KumarGarlapati, V., Shankar, U., Budhiraja, A., 2016. Bioconversion technologies of crude glycerol to value added industrial products. Biotechnol. Reports 9, 9–14.

Lu, J., Liu, Z., Zhang, Y., Li, B., Lu, Q., Ma, Y., Shen, R., Zhu, Z., 2017. Improved production and quality of biocrude oil from low-lipid high-ash macroalgae Enteromorpha prolifera via addition of crude glycerol. J. Clean. Prod. 142, 749–757. https://doi.org/10.1016/j.jclepro.2016.08.048.

Maglinao, R.L., He, B.B., 2009. Thermal Conversion of Glycerol to Primary Alcohols Using a Batch Pressure Reactor. ASABE Meet. Pap. 0300.

Mariotti, F., Tomé, D., Mirand, P.P., 2008. Converting Nitrogen into Protein — Beyond 6. 25 and Jones ' Factors Converting Nitrogen into Protein — Beyond 6. 25 and Jones ' Factors. Crit. Rev. Food Sci. Nutr. 48, 177–184. https://doi.org/10.1080/10408390701279749.

Peterson, A.A., Vogel, F., Lachance, R.P., Fröling, M., Antal, M.J., Tester, J.W., 2008. Thermochemical biofuel production in hydrothermal media: a review of sub- and supercritical water technologies. Energy Environ. Sci. 1, 32–65. https://doi.org/10.1039/b810100k.

Reza, H., Shekouhy, M., Sha, V., Davoodi, M., 2013. Glycerol based ionic liquid with a boron core: a new highly efficient and reusable promoting medium for the synthesis of quinazolinones. J. Mol. Liq. 180, 139–144. https://doi.org/10.1016/j.molliq.2013.01.013.

Sato, N., Quitain, A.T., Kang, K., Daimon, H., Fujie, K., 2004. Reaction kinetics of amino acid decomposition in high-temperature and high-pressure water. Ind. Eng. Chem. Res. 43, 3217–3222. https://doi.org/10.1021/ie020733n.

Selvaratnam, T., Pegallapati, A.K., Reddy, H., Kanapathipillai, N., Nirmalakhandan, N., Deng, S., Lammers, P.J., 2015. Algal biofuels from urban wastewaters: maximizing biomass yield using nutrients recycled from hydrothermal processing of biomass. Bioresour. Technol. 182, 232–238. https://doi.org/10.1016/j.biortech.2015.01.134.

Smarrito-menozzi, C., Matthey-doret, W., Devaud-Goumoens, S., Viton, F., 2013. Glycerol, an underestimated flavor precursor in the maillard reaction. J. Agric. Food Chem. 61, 10225–10230.

Sudasinghe, N., Dungan, B., Lammers, P., Albrecht, K., Elliott, D., Hallen, R., Schaub, T., 2014. High resolution FT-ICR mass spectral analysis of bio-oil and residual water soluble organics produced by hydrothermal liquefaction of the marine microalga Nannochloropsis salina. Fuel 119, 47–56. https://doi.org/10.1016/j.fuel.2013.11.019.

Sudasinghe, N., Reddy, H., Csakan, N., Deng, S., Lammers, P., Schaub, T., 2015. Temperature-dependent lipid conversion and nonlipid composition of microalgal hydrothermal liquefaction oils monitored by fourier transform ion cyclotron resonance mass spectrometry. Bioenergy Res. 8, 1962–1972. https://doi.org/10.1007/s12155-015-9635-9.

Tendam, J., Hanefeld, U., 2011. Renewable chemicals: dehydroxylation of glycerol and polyols. ChemSusChem 4, 1017–1034. https://doi.org/10.1002/cssc.201100162.

Wu, M., Ma, C., Yang, C., Kao, W., Shen, S., 2011. The formation of IQ type mutagens from Maillard reaction in ethanolic solution. Food Chem. 125, 582–587. https://doi.org/10.1016/j.foodchem.2010.08.067.

Yang, F., Hanna, M.A., Sun, R., 2012. Value-added uses for crude glycerol - A byproduct of biodiesel production. Biotechnol. Biofuels 5, 13. https://doi.org/10.1186/1754-6834-5-1322413907.

Yang, T., Jie, Y., Li, B., Kai, X., Yan, Z., Li, R., 2016. Catalytic hydrodeoxygenation of crude bio-oil over an unsupported bimetallic dispersed catalyst in supercritical ethanol. Fuel Process. Technol. 148, 19–27. https://doi.org/10.1016/j.fuproc.2016.01.004.

Ye, Z., Xiu, S., Shahbazi, A., Zhu, S., 2012. Co-liquefaction of swine manure and crude glycerol to bio-oil: model compound studies and reaction pathways. Bioresour. Technol. 104, 783–787. https://doi.org/10.1016/j.biortech.2011.09.126.

Yuan, X.Z., Li, H., Zeng, G.M., Tong, J.Y., Xie, W., 2007. Sub- and supercritical liquefaction of rice straw in the presence of ethanol-water and 2-propanol-water mixture. Energy 32, 2081–2088. https://doi.org/10.1016/j.energy.2007.04.011.

Zhang, C., Tang, X., Sheng, L., Yang, X., 2016. Enhancing the performance of Co-hydrothermal liquefaction for mixed algae strains by the Maillard reaction. Green Chemistry. https://doi.org/10.1039/c5gc02953h.

Zhang, J., Zhang, Y., 2014. Hydrothermal liquefaction of microalgae in an ethanol-water Co-solvent to produce biocrude oil. Energy and Fuels 28, 5178–5183. https://doi.org/10.1021/ef501040j.